Soliton switching in ferroelectric liquid crystals and their transient electro-optic response

I. Abdulhalim[a)]
Optoelectronics Research Center, Optical Fiber Group, Southampton University, Highfield, Southampton SO9 5NH, United Kingdom

G. Moddel and N. A. Clark
Optoelectronic Computing Systems Center, University of Colorado, Boulder, Colorado 80309-0425

(Received 21 January 1994; accepted for publication 4 April 1994)

The switching behavior of ferroelectric liquid crystals (FLCs) is studied both experimentally and theoretically. Experimentally the electro-optic response of multiwavelength-thick FLC cells revealed transient peak and dip characteristics. This behavior could not be explained at all according to the standard picture of a switchable birefringent plate, nor according to transient light scattering associated with ferroelectric domain reversal. Solutions of a numerical model of the FLC electric and elastic torques, which results in the sine-Gordon equation, showed the propagation of kink-antikink pair solitons. The nonuniform director structures corresponding to these solitons are sufficient to explain the experimental behavior of the transient electro-optic response with the wavelength, the field, and the polarizer-cell-analyzer orientation. The electro-optic response is found to be highly sensitive to the fixed boundary dipole orientations.

I. INTRODUCTION

Ferroelectric liquid crystals (FLCs) exhibit a variety of structures depending on their interaction with the aligning solid boundaries, the aligning procedure, and the applied external fields.[1] The behavior of these FLC structures under an applied electric field $\mathbf{E}$ is of particular importance both because they can appear in any of the current FLC devices and because they exhibit interesting physical phenomena. The common operational mode of FLC cells is the one in which a bipolar electric field is applied in the plane of the molecular layers. Upon the sign reversal of an electric field, the molecular dipoles $\boldsymbol{\mu}$ flip between two states, say up and down, and associated with that is the director reorientation $\mathbf{n}$. The nature of the polarization-director field configuration $(\mathbf{n}-\mathbf{p})$ during the switching depends on the strength of the field and the strength of the anchoring to the solid plates through the aligning layers. For the case of zero anchoring, the dipoles are free to reorientate with the field and the transient structure is uniform. Optically, the FLC cell in this case acts as a switchable birefringent plate. For the case of finite but nonzero anchoring, the elastic forces cause the transient structure to be nonuniform, depending on the field strength, the initial structures, and the anchoring energy.

In a previous letter[2] we reported on a new electro-optic (EO) effect in which the transient electro-optic response of FLCs was found to exhibit strong dependence on the wavelength and the fixed boundary dipole orientations. The simulations agreed best with the experimental results for a FLC alignment such that the boundary dipoles are slightly off the surfaces normal. The switching in this case proceeds via the excitation of solitons in the form of sine-Gordon kink-antikink pairs which propagate toward, and collide near, the center of the cell where they annihilate. The purpose of this article is to present a detailed study of the experimental observations and the theoretical calculations for the dynamics and the optics of the transient nonuniformities of fixed boundary FLCs.

II. EXPERIMENTAL AND OBSERVATIONS

The FLC cells considered are planarly aligned between two optically flat glass substrates where the molecular layers are in the bookshelf geometry (Fig. 1). The glass substrates are coated with thin layers (~700 Å) of transparent conducting oxide (TCO) electrodes and aligning layers. The FLC material filled the gap between the two substrates by capillary action in the isotropic phase under vacuum, and was then cooled slowly to the ferroelectric phase at room temperature to maintain alignment. The thickness of the FLC layer is controlled using glass bead spacers. The aligning layers prepared either by oplique evaporation of SiO_x or using the rubbed polymer alignment technique. Among the LC materials which were investigated are CS1014, CS1017, CS1026, SCE9, SCE12, SCE10, and ZLI3654, (the series CS are products of Chisso corporation, and SCE and ZLI are of Merck Ltd). Although the results we present here are from cells prepared using the unidirectional rubbing of the polymer nylon 6/6, similar behavior was observed on a variety of cells prepared using different polymers, different LC materials, and also using the SiO_x aligning technique. The cells did not show complete extinction of white light when viewed under the microscope between two crossed polarizers. This observation indicates a splay nonuniformity of the as-prepared cells. There were no indications of chevron structures in the majority of the cells. The LC material SCE10 does not exhibit the SmA^* phase and passes directly from the nematic to the SmC^* phase. The results reported are from a 10-μm-thick cell of CS1014 which transforms from the isotropic to the nematic phase at 81 °C, to the SmA phase at 69 °C, and to the ferroelectric phase at 54 °C.

[a)]Presently with: KLA Instruments Corp., 4 Science Ave., P.O. Box 143, Migdal Hae'mek 10500, Israel.

 0021-8979/94/76(2)/820/12/$6.00

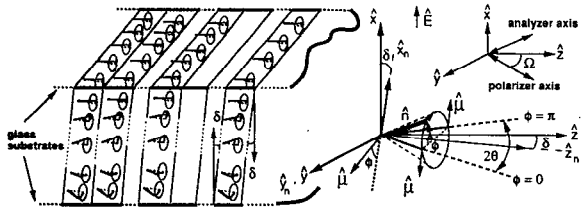

FIG. 1. The experimental setup and the geometry of the planarly aligned FLC cells used in this study. The molecular layers are in the bookshelf geometry where their normal Z_n can be tilted by an angle δ from the plane of the substrates YZ. The molecular orientation is identified by the azimuth angle $\phi(x)$ and the tilt angle θ. The two principal refractive indices are along the molecular director $n_\parallel$ and perpendicular to it $n_\perp$. The local molecular dipoles which contribute to the ferroelectric polarization density are designated by μ. The electric field $\mathbf{E}$ is applied along the normal to the substrates X. The polarizer plane is parallel to the substrate plane and its axis makes an angle Ω with respect to the projection of the normal to the layers on the substrate plane YZ. The angle Ω defines the cell orientation. The coordinates system $X_nY_nZ_n$ is obtained from the XYZ system by rotation around the Y axis by the pretilt angle δ.

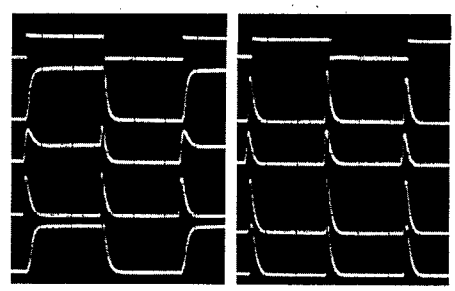

FIG. 2. (a) Oscilloscope traces showing the electro-optic response to a bipolar field pulses (upper trace) with the $\Omega=\theta$ geometry at different wavelengths from top to bottom: 637, 593, 524, and 481 nm, respectively. The cell is CS1014, 10 μm thick. The applied electric-field pulses are symmetric with a peak-to-peak voltage of $V_{pp}=200$ V and frequency 100 Hz. (b) The dependence of the pure transient peak height obtained in (a), with $\lambda=524$ nm, on the cell orientation. Apart from small variations in the peak height, the peak persists at any orientation of the cell. The cell orientations with respect to the $\Omega=\theta$ position are from top to bottom 0°, 45°, 70° and 90°.

We measured the light transmittance through the cells between two crossed polarizers at different wavelengths in response to a symmetric bipolar field pulses. The wavelength was varied continuously using a computer-controlled Spex monochromator with a resolution of 2 nm. The transmitted light was measured using a photomultiplier and an oscilloscope. The usual and desired EO response of FLCs is the one in which the transmittance is very small (ideally zero) during one cycle of the applied pulse (say negative) and very high (ideally 100%, ignoring losses due to the polarizers) during the positive cycle. This situation can be achieved when the polarizer axis is along the projection of the molecular director $\mathbf{n}$ on the YZ plane in the $\phi=0$ state (Fig. 1). The angle which the projection of $\mathbf{n}$ on the YZ plane makes with respect to the Z axis is

$$\alpha=\arctan[\sin\theta\cos\phi/(\cos\delta\cos\theta + \sin\delta\sin\theta\sin\phi)].$$

The above geometry is then achieved when $\phi=0$ and hence $\Omega=\alpha=\arctan(\tan\theta/\cos\delta)$. Because for small δ we have $\alpha=\theta$ then throughout this article we refer to this geometry as the usual response or the $\Omega=\theta$ geometry. After a high enough negative field is applied, the projection of the optic axis on the polarizer plane is along the polarizer axis and ideally complete extinction is observed (off state) if the field is high enough that the structure is almost uniform.

Upon reversing the polarity of the field to positive, the projection of the optic axis is rotated by $2\Omega\approx\pi/4$ and some light is transmitted depending on the thickness and the wavelength, $T=\sin^2(\pi d\Delta n/\lambda)\sin^2(4\Omega)$, where $\Delta n=n_e-n_0$ is the effective birefringence. The expression for the extraordinary refractive index for any ϕ is given by

$$n_e=n_\parallel n_\perp/(\epsilon_\parallel\sin^2\gamma+\epsilon_\perp\cos^2\gamma)^{1/2},$$

where

$$\gamma=\arcsin(\cos\delta\sin\theta\sin\phi-\sin\delta\cos\theta),$$

and the ordinary refractive index is $n_0=(\epsilon_\perp)^{1/2}$. For small δ the effective birefringence in the two states $\phi=0$ and π is the molecular birefringence $\Delta n_m=(\epsilon_\parallel)^{1/2}-(\epsilon_\perp)^{1/2}$. When λ satisfies the multi-half-wave-plate (MHWP) condition $d=(2m-1)\lambda/2\Delta n_m$ $(m=1,2,...)$, the transmittance is 100% while it vanishes when the multi-full-wave-plate (MFWP) condition $d=m\lambda/\Delta n_m$ is satisfied. Figure 2(a) shows the EO response with this geometry at different wavelengths of a 10-μm-thick cell made of CS1014 and peak-to-peak applied voltage of $V_{pp}=200$ V. At $\lambda=637$ nm (MHWP with $m=3$) the EO response is the usual one with a contrast ratio of 120:1. As the wavelength changes, peaks start to appear during the sign reversal of the bipolar field. At $\lambda=524$ nm the EO response consists only of the transient peaks, while the transmittance levels during the positive and negative cycles of the field are equal and close to zero. The height of the transient peaks is the same as that of the on state in the usual response trace. The next wavelength at which the usual response is obtained is $\lambda=481$ nm (MHWP with $m=4$) as shown in the lowest trace of Fig. 2(a). The pure transient peak appears again at $\lambda=431$ nm (not shown). Note that the wavelengths at which the pure transient peaks appear satisfy the MFWP condition with $m=3$ and 4 for $\lambda=524$ and 431, respectively. This is expected since these are the wavelengths at which the transmittance levels during the positive and negative cycles of the field become equal and close to zero.

The phenomena we are considering here are related to the shape of these transient peaks, their time evolution, and their dependence on the wavelength, the field, and the cell orientation. First we point out that when pure peaks are obtained, they do not depend on the cell orientation, apart from small variations in their height [Fig. 2(b)]. At very small fields they can become more structured, wide, and very often they become dips rather than peaks [Fig. 3(a)]. They start to be pure peaks above a certain field, then grow in height until reaching a maximum then they decay and saturate [Fig. 3(a)]. When the wavelength corresponds to that which yields the regular EO response (MHWP), dips appear when the cell is orientated to the position $\Omega=0$ (Fig. 1) while the transmittance levels during the positive and negative cycles of the fields are equal and close to 50% (Fig. 4); however, the pure

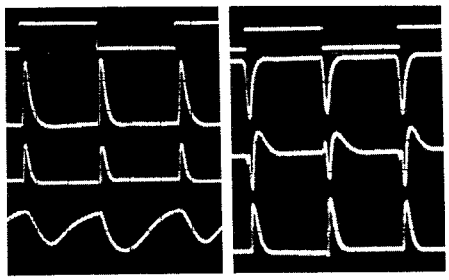

(a) (b)

FIG. 3. (a) Variation of the pure transient peak with the applied peak-to-peak voltage. $\lambda=524$ nm, with the $\Omega=0$ geometry and the three lower traces correspond to peak-to-peak voltages of 3, 7, and 0.1 V/μm, from top to bottom, respectively. (b) The experimental transient EO response in the high-field limit $E=4$ V/μm and the $\Omega=0$ geometry at different wavelengths showing the transition from a pure peak at λ which satisfies the MFWP condition (lowest trace) and the pure dip when λ satisfies the MHWP condition (second trace from top) and at λ in between the two conditions (third trace from top).

peaks appear again with the previous orientation when λ satisfies the MFWP condition (Fig. 4).

These observations show that the transient EO response cannot be explained in terms of a switchable birefringent plate (SBP). According to the model of SBP, when λ satisfies the MFWP condition in the $\Omega=\theta$ geometry, a pure peak should appear during the switching due to the change in the effective birefringence with ϕ; however, this peak height is much smaller than the observed one and also it should not exhibit the same observed dependence on the cell orientation and the voltage. With the $\Omega=0$ geometry, for instance, the peak should split into two, because when the molecular director arrives to the midpoint $\phi=\pi/2$ on the tilt cone, its projection on the polarizer plane is along the polarizer axis and therefore an extinction should occur at that instant. Similarly, the transient scattering[3,4] due to random domain inversion cannot explain these observations because the scattering does not have such a strong dependence on the wavelength, the field, and the cell orientation. These facts led us to believe that nonuniform structures evolve during the switching

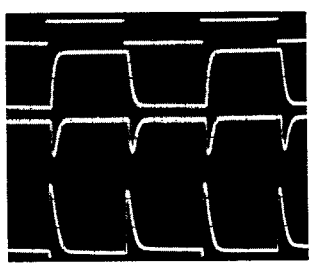

FIG. 4. Upper trace is the applied bipolar pulses with $V_{pp}=50$ V and frequency 100 Hz. Second trace from top is due to $\Omega=\theta$ geometry with $\lambda=637$ nm. Third from top is the same as the second with the orientation $\Omega=0$ and the lowest trace is the same orientation as the third with different wavelength $\lambda=525$ nm. This figure demonstrates that the transmittance levels are the same during the positive and the negative field intervals in the $\Omega=0$ geometry and equal to 50% of the level obtained in the $\Omega=\theta$ geometry when λ satisfies the MHWP condition. On the other hand the transient peak height is equal to 100% when λ satisfies the MFWP condition.

in response to a bipolar field. Because the transient peaks persist for any high field, we infer that the boundary dipole orientations are not changing with the field strength. Otherwise, above a certain field, which is able to switch the boundary dipoles, the EO response should become that of a SBP. These speculations led us to consider the dynamics of FLCs with fixed boundary orientations.

III. BIPOLAR SWITCHING VIA SINGLE SOLITON

Most of the as-prepared FLC cells which exhibit the transient behavior described in the previous section do not show any extinction position of white light when viewed between two crossed polarizers with no field applied. Some color exists, although being weak, it indicates the existence of nonuniform structure, most likely a linearly splayed profile $\phi(x)=qx+\phi_1$ with $q=(\phi_2-\phi_1)/d$, where $\phi_1,\phi_2=\pi-\phi_1$ are the boundary dipole orientations. The assumption that the splay is linear is not crucial in the case of bipolar switching because once a high enough field is applied the nature of the final structure depends mainly on the fixed boundary orientations ϕ_1 and ϕ_2. The first case we consider is that with the boundary dipoles being perpendicular to the normal to the surfaces. Although the dynamics in this case were reported previously,[5] it is presented here because we present for the first time the EO response associated with it and also because it is important for the understanding of the subsequent cases. In the one elastic constant approximation, the dynamic equation governing the director-polarization orientation is the double overdamped sine-Gordon equation,

$$\tau_f \frac{\partial\phi}{\partial t}=\xi_s^2\frac{\partial^2\phi}{\partial x^2}\pm\sin\phi + \left(\frac{E\Delta\epsilon\sin^2\theta\cos\delta}{4\pi P}\right)\cos\phi(\sin\phi-\sin\phi_1). \tag{1}$$

Here $\tau_f=\eta_\phi/PE\cos\delta$ is the ferroelectric characteristic time and $\xi_s=(K_s/PE\cos\delta)^{1/2}$ is the ferroelectric coherence length, where η_ϕ is the rotational viscosity associated with ϕ motion, K_s is the splay elastic constant, $\Delta\epsilon$ is the dielectric anisotropy, θ is the molecular tilt angle, and δ is the layer pretilt angle given by $\tan\delta=\sin\phi_1\tan\theta$. Numerical integration of Eq. (1) was performed using Gear's finite difference technique[6] with 1000 mesh points, different fixed boundary conditions ϕ_1,ϕ_2 and different initial profiles $\phi(x,0)$. The material parameters used in the calculations are $\theta=\pi/8$, $P=10$ nf/cm^2, $\Delta\epsilon=-1$, $\eta_\phi=0.016$ P, and $K_s=10^{-7}$ erg/cm. A negative step potential was applied first for a time interval $t_-=20$ ms and we calculated the profile $\phi(x,t_-)$ at the end of this time interval. This later profile represents the $(-)$ state. Then the field sign was reversed instantaneously and the profile $\phi(x,t_-)$ was taken as the initial data for the calculated profiles $\phi(x,t)$ during the switching.

The time evolution of $\phi(x,t)$ during the $(-)$ cycle for different fields and the case of $\phi_1=0$ is shown in Figs. 5(a)–5(c). For the case of small fields [Fig. 5(a)], the nonlinear terms in Eq. (1) are small compared to the elastic and damping terms. The field causes some distortion but it is not able

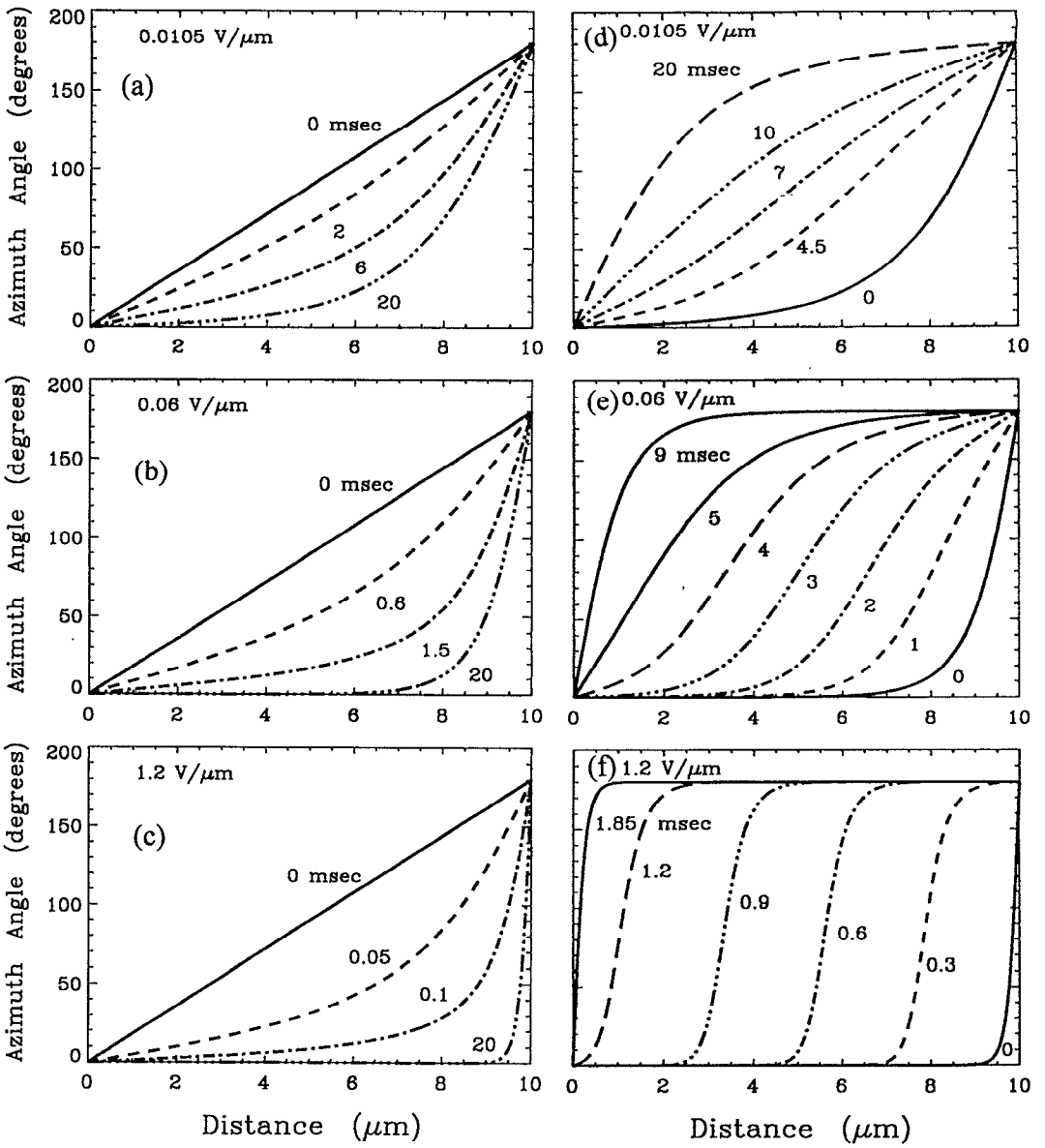

FIG. 5. (a)–(c) Evolution of the azimuth angle profiles $\phi(x,t)$ in response to a monopolar negative step potential for a period of $t_-=20$ ms with different heights. The initial profile is linearly splayed with the fixed boundary orientations, $\phi_1=0°$ and $\phi_2=\pi$, and cell thickness $d=10$ μm. (d)–(f) Evolution of $\phi(x,t)$ after reversing the field polarity on the profiles $\phi(x,t_-)$ of (a)–(c). The profiles $\phi(x,0)$ in (d)–(f) are the same as the profiles $\phi(x,t_-=20$ ms) in (a)–(c).

to switch all of the dipoles completely. This is the case of small distortion regime where an approximate analytic solution can be found,

$$\phi(x,t)\simeq qx+(\tau_e/\tau_f)[1-\exp(-t/\tau_e)]\sin qx+\phi_1. \quad (2)$$

This profile is characterized by the existence of a characteristic elastic frequency $1/\tau_e$ and a characteristic elastic time $\tau_e=\eta_\phi/q^2K_s$ which does not depend on the field. As the field increases, larger fraction of the dipoles switch completely and the profile $\phi(x,t_-)$ becomes sharper [Fig. 5(b)]. Above a certain field the majority of the dipoles switch completely except for a thin localized layer near the boundary which connects the dipoles at the boundary $x=d$ to the bulk [Fig. 5(c)]. This layer can be described by the static sine-Gordon kink,[7]

$$\phi(x,0)=2\arctan[\exp(x-d)/\Delta]. \quad (3)$$

Here $\Delta\propto 1/|E|^{1/2}$ is the width of the kink. Upon reversing the field polarity in the end of the time interval $t_-=20$ ms, the initial profiles used in the calculation are now the profiles obtained after $t_-=20$ ms in Figs. 5(a)–5(c), and are now labeled $t=0$ in Figs. 5(d)–5(f). In the small field regime the profile $\phi(x,t)$ oscillates linearly around the linearly splayed profile. As the field increased the deviation from the linear oscillations case increases. For the case when the profile at $t=0$ satisfies the sine-Gordon kink solution of Eq. (3) [Fig. 5(e)], the switching proceeds via the propagation of this kink in the negative x direction with constant velocity v, and shape represented by the solution[8]

$$\phi(x,t)=2\arctan\{\exp[(x+vt-d)/\Delta]\}. \quad (4)$$

Physically, the switching proceeds via the motion of this solitary wave because its speed is so high that it can propa-

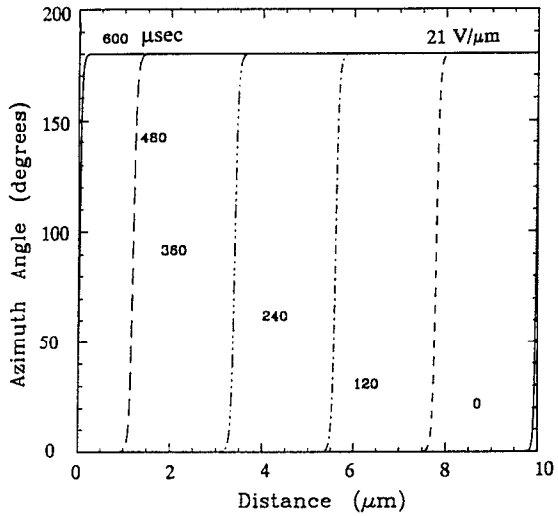

FIG. 6. Evolution of $\phi(x,t)$ after the sign reversal of the applied field as in Figs. 5(d)–5(f), but for very high field to demonstrate the sharpness and the higher speed of the single excited soliton.

gate through the whole cell within a time d/v, shorter than the delay time of any of the dipoles outside the static initial kink region. This is the physical origin for the existence of a threshold field above which a soliton is excited. Therefore, the higher their speed, the longer the distance they can travel without distortion and collapse if the dipoles outside the static kink region have a finite delay time. Since the delay time diverges logarithmically as the dipoles approach the $\phi=0$ orientation, there will be no collapse of the travelling kinks for any thick cell if the field is high enough. Because of the fixed dipole orientation on the boundary $x=0$, the kink will slow [Fig. 5(c)] as it approaches this boundary. Figure 6 illustrates how thin and fast the travelling kink becomes for high fields.

IV. THE EO RESPONSE ASSOCIATED WITH SINGLE SOLITON EXCITATION

The optical properties of the splayed nonuniform profiles of Figs. 5(a)–5(c), in response to a monopolar and bipolar fields and the propagation of an electromagnetic wave through the kink region, are of particular interest. They reveal unique features of the EO response which can help in understanding the as-prepared structure of FLCs and in designing new EO devices. Since the aim of this article is to clarify the switching via solitary waves, we refer the reader to previous articles[9,10] for more details on the optics of splayed FLC structures. The nonuniform splayed FLC layers were shown to have a strong effect[10] on the EO response and their existence allows for continuous phase-only and amplitude light modulation.[9] The transmittance through our FLC cells during the switching as a function of time was calculated at constant wavelength with the geometries of Fig. 1. The calculation of the transmittance is based on the 4×4 matrix method,[11] and the procedure for calculating the propagation matrix for one thin slab (which corresponds to one

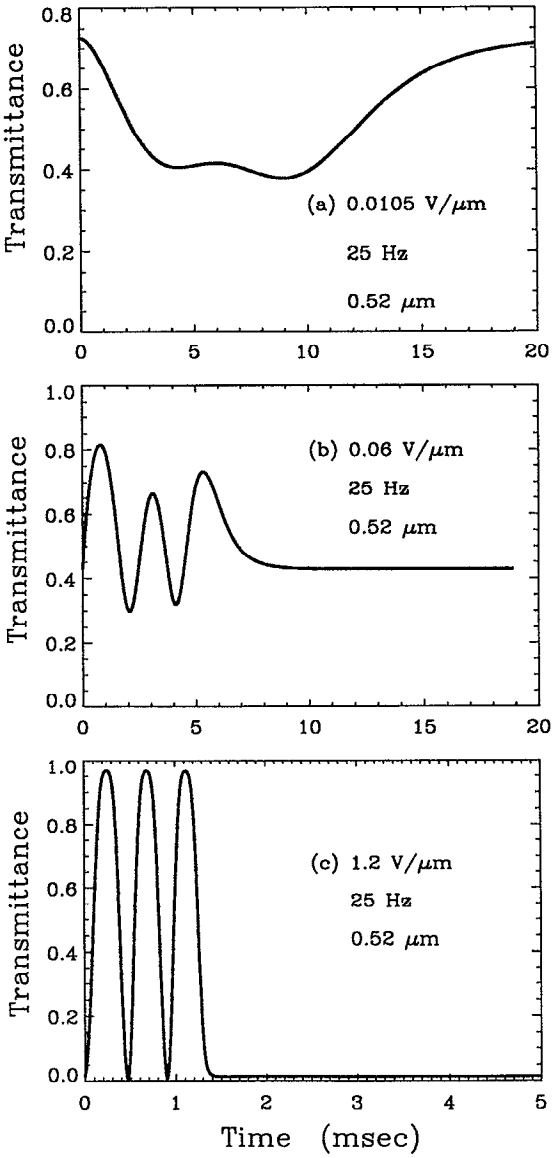

FIG. 7. The transient electro-optic response associated with the time evolution of $\phi(x,t)$ in Figs. 5(d)–5(f) for the $\Omega=0$ geometry and $\lambda=0.52$ μm, which satisfies the MFWP condition.

mesh point) uses the Lagrange–Sylvester interpolation polynomial described elsewhere.[12] The molecular refractive indices are $n_{\parallel}=1.66$ and $n_{\perp}=1.5$.

The transmittance time evolution which corresponds to the transient switching in Figs. 5(d)–5(f) is shown in Figs. 7(a)–7(c), respectively, for the geometry $\Omega=0$. The wavelength was selected to satisfy the MFWP condition. The optical parameters of the LC material correspond to those of CS1014 since most of our measurements were performed on this material. In the low-field regime the transient transmittance consists of a dip in agreement with the experiment. As the field increases three peaks start to appear, and when the switching proceeds by the motion of a single soliton the transient pattern consists of three identical peaks. The height of the peaks saturate at 100% transmittance for high fields but they become narrower as shown in Fig. 8(a). As the

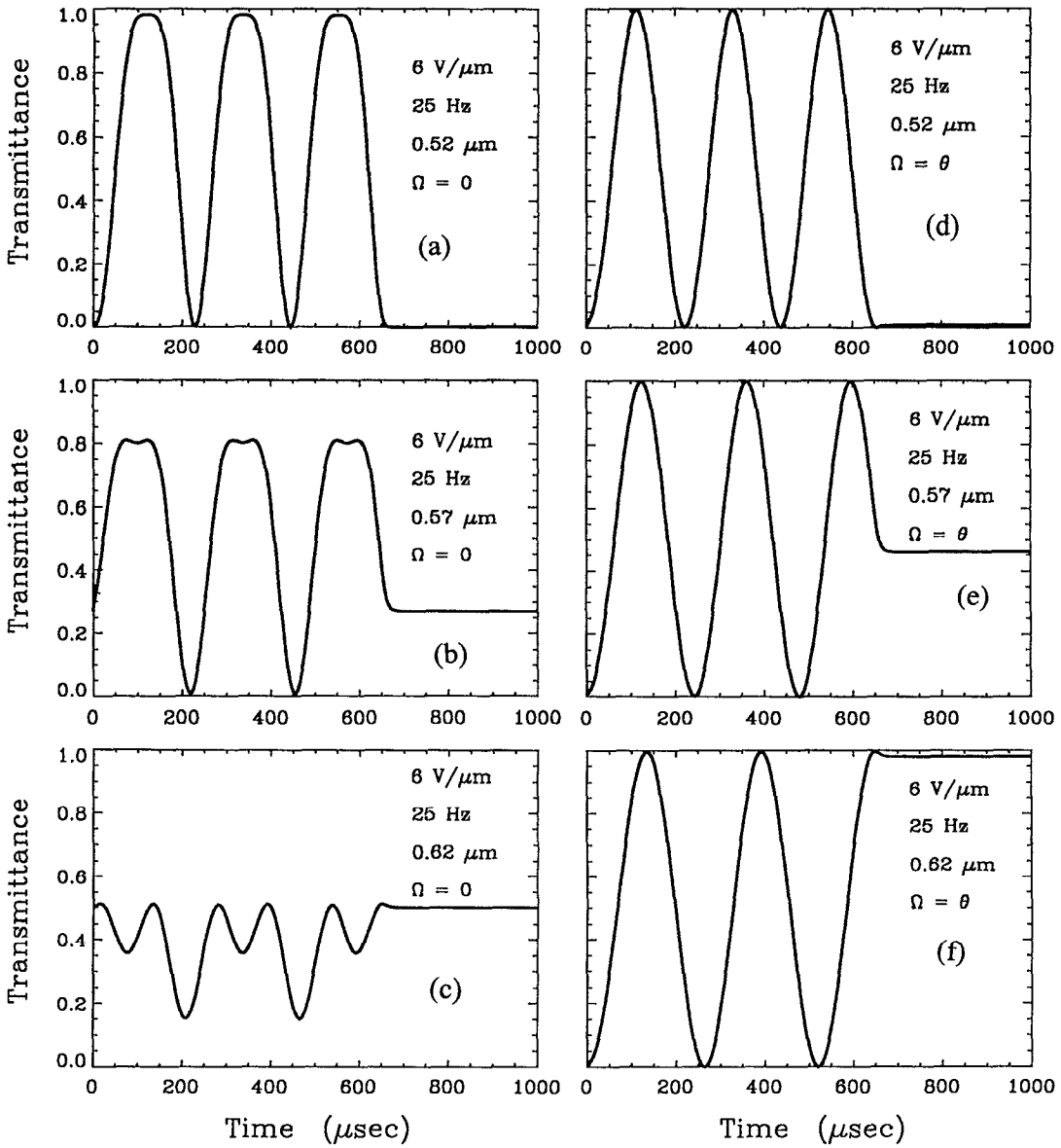

FIG. 8. (a)–(c) The transient EO response associated with the motion of a single soliton at higher field and different wavelengths starting from $\lambda=0.52$ μm, which satisfies the MFWP condition, up to $\lambda=0.62$ μm, which satisfies the MHWP condition for the $\Omega=0$ geometry. (d)–(f) Same conditions as in (a)–(c) but for the $\Omega=\theta$ geometry.

wavelength is varied to satisfy the MHWP condition, the initial and final transmittance levels become equal to 50% as expected since the two states $\phi(x,t)$ and $\phi(x,t_+)$ are equivalent optically when the field is high enough. In fact, this optical symmetry exists with the $\Omega=0$ geometry no matter what the field strength is and for any wavelength, as is seen also in Fig. 7. In the low-field regime this is because the phase of the emerging electromagnetic wave depends quadratically on the field, as was shown recently.[9] In the high-field regime, the optical symmetry is expected because in this case the only nonuniform layers are the two thin ones near the two boundaries obtained at $t=t_-$ and $t=t_+$. Since these layers are much thinner than the wavelength of light, the structure behaves as a uniform structure so that, with the $\Omega=0$ geometry, the optical symmetry is expected. Figures 8(d)–8(f) show how the transmittance of Figs. 8(a)–8(c) varies when the cell is oriented to $\Omega=\theta$. The three peaks pattern persists when λ satisfies the MFWP condition, but two identical peaks appear before the final transmittance level (100%) is achieved when λ satisfies the MHWP condition [Fig. 8(f)].

Although the calculated transient EO response in the case of a single soliton excitation exhibits a complicated pattern which shows how the transient nonuniformities can affect strongly the EO response, it does not explain the experimental observations. The number of transient peaks is not the only discrepancy, since the three peaks can be reduced to one depending on the ratio d/λ of the thickness to the wavelength. Experimentally the number of transient peaks observed is independent of the ratio d/λ. Furthermore, the calculated transient peaks do not explain the observed dependence on the field and the cell orientation. Before we proceed further in considering the double-kink case to ex-

plain the experimental observations, we would like to explain first the transient peaks obtained in the single soliton case. For that purpose, we consider the high-field regime where the width Δ of the propagating kink is much shorter than the wavelength of light ($\Delta \ll \lambda$) so that the kink acts only as a thin boundary separating two uniform birefringent plates. One of the two plates has a thickness $d_k = vt$ formed by the distance traversed by the kink during the time t which is orientated at $\phi = \pi$, and the other is the remaining part of the cell $d_r = d - d_k$ orientated at $\phi = 0$. The transmittance through such a system of two birefringent plates between two crossed polarizers exhibits maxima and minima when the thickness d_k is varied with time. Their total number depends on the total thickness d and the wavelength. When the wavelength satisfies the MFWP condition with order m, that is $\lambda = d\Delta n_m/m$, the transmittance in the geometry of $\Omega = 0$ is given by

$$T = \sin^2 2\theta[\sin^2 \Gamma_k + 4 \cos^2 2\theta \sin^4(\Gamma_k/2)], \quad (5)$$

where $\Gamma_k = 2\pi d_k \Delta n_m/\lambda$. For $\theta \approx \pi/8$ we get $T = 100\%$ when $\Gamma_k = (2l-1)\pi$, and $T = 0$ when $\Gamma_k = 2l\pi$ where $l = 1,2,\ldots$. Hence, the peaks are obtained when the kink traverses distances which satisfy $d_k = (2l-1)\lambda/2\Delta n_m$ or using $\lambda = d\Delta n_m/m$ we obtain

$$d_k = (2l-1)d/2m. \quad (6)$$

Since $d_k < d$, the maximum number of peaks for certain m is $l_{\max} = m$. In the case presented in Figs. 7 and 8(a)–8(c) we had $\lambda = 0.52$ μm, $\Delta n_m = 0.16$, and $d = 10$ μm which yields $m = 3$, in agreement with the numerical calculations. For smaller thicknesses and different wavelengths we confirmed that, depending on the ratio d/λ, a single peak is obtained. For cells thinner than 4 μm only one peak is obtained because of the restriction on m for λ in the visible range. Therefore, if only the number of peaks is compared to the experiment, one can be misled into thinking that the transient EO response of thin cells has been modeled adequately with a single soliton. Their behavior with the different parameters had to be considered.

V. KINK-ANTIKINK PAIR PRODUCTION AND ANNIHILATION

When the dipole orientations at the two boundaries $x = 0$ and $x = d$ are off the normal to the substrates then $\phi_1 \neq 0$ and $\phi_2 = \pi - \phi_1$. This situation can occur as a result of layer pretilt in all the smectic layers or simply pretilt of only the boundary dipoles. Upon applying a high enough negative field the dipoles located away from the boundaries and within the range $d - 2\xi_s$ will switch completely after a long enough time. The dipoles near the boundaries within a distance ξ_s form thin nonuniform layers which connect the central region of the cell oriented at $\phi = 0$ to the fixed dipole orientations ϕ_1 and ϕ_2 at the boundaries $x = 0$ and $x = d$, respectively [Fig. 9(a)]. When these nonuniform interface layers satisfy the static kink-type solution given in Eq. (3), then by reversing the field polarity, two solitons are expected to be generated. The two thin layers near the two boundaries formed before reversing the field polarity can be shown to be described by

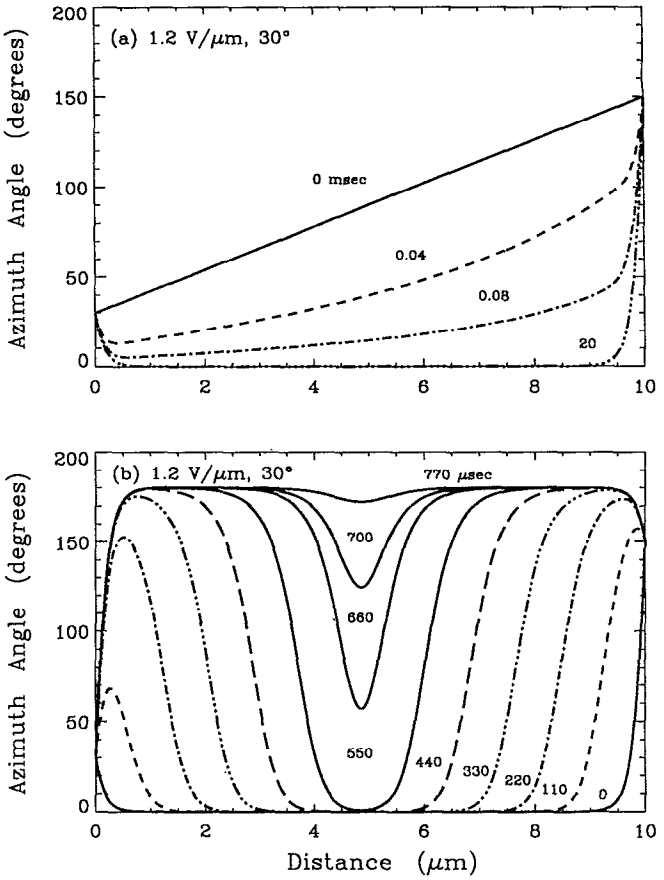

FIG. 9. (a) Evolution of $\phi(x,t)$ in response to a monopolar negative step potential for initially linearly splayed structure with fixed boundary orientations $\phi_1 = 30°$ and $\phi_2 = 150°$ with a field high enough to produce static sine-Gordon kinks near the two boundaries after $t_- = 20$ ms. (b) Evolution of $\phi(x,t)$ after reversing the sign of the field in (a) after t_- demonstrating the excitation of a kink-antikink pair, their motion at the same speed, and in opposite directions until colliding near the center of the cell and annihilating each other.

$$\phi(x,0) = 2 \arctan[\tan(\phi_1/2)\exp(-x/\Delta)]$$

for the layer located near $x = 0$, and

$$\phi(x,0) = 2 \arctan\{\tan(\phi_2/2)\exp[(x-d)/\Delta]\}$$

for the layer located near $x = d$. Upon reversing the field polarity, the dipoles which switch first to the up orientation are those with the shortest delay times, i.e., the ones next to the fixed dipoles at the boundaries. When these dipoles switch completely, then traveling domain walls are created [Fig. 9(b)]. These domain walls have the same shape as in the single-kink case [Figs. 5(f) and 6] and are characterized by the traveling-wave solution of Eq. (4). The kink near the boundary $x = d$ is formed before the one near $x = 0$ because $\phi_2 > \phi_1$. Because their profiles $\phi(x,t)$ have slopes with opposite signs and because they travel in opposite directions, they are called a kink-antikink pair. The case shown in Fig. 9 corresponds to relatively high deviation of the boundary dipoles from the surfaces normal, $\phi_1 = 30°$ and $\phi_2 = 150°$. This is not the case which explains the experimental observations, but is shown to demonstrate clearly the existence of two

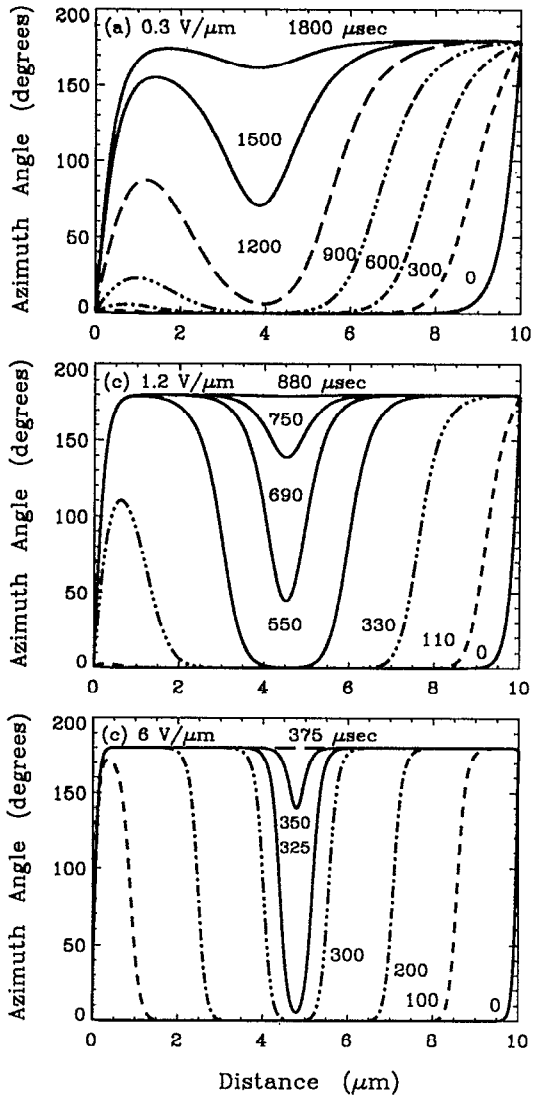

FIG. 10. Evolution of $\phi(x,t)$ after the sign reversal of a negative field applied to a linearly splayed profile with $\phi_1=1°$ and $\phi_2=179°$ for $t_-=20$ ms, demonstrating double soliton excitation above a high enough field.

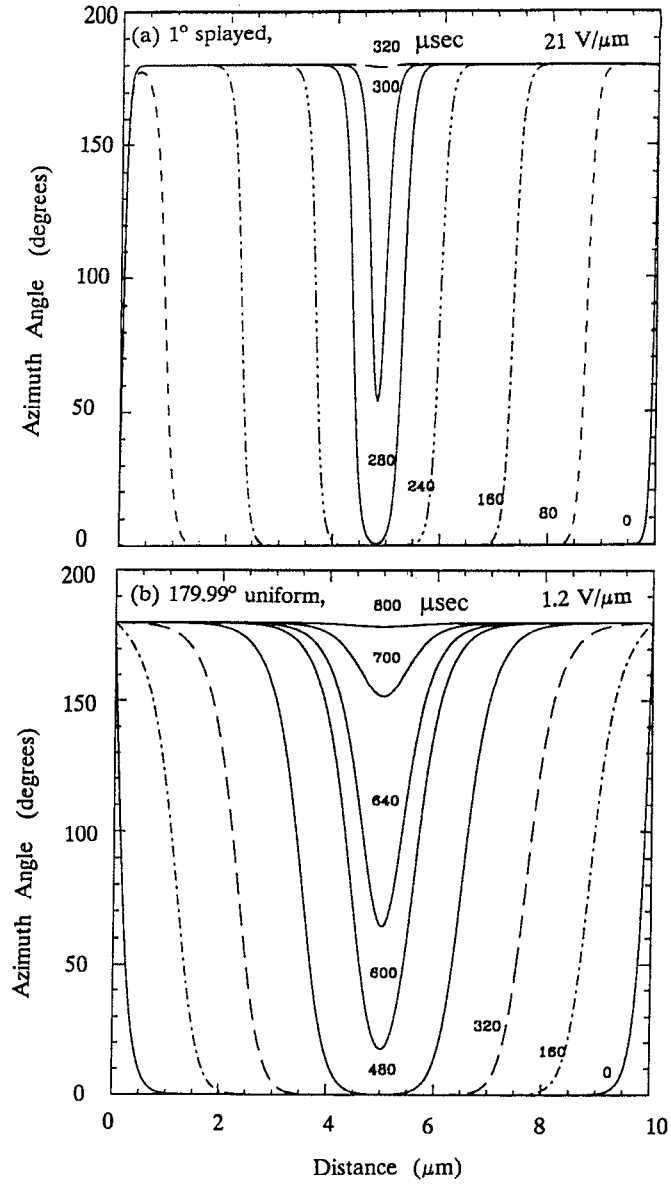

FIG. 11. (a) Evolution of $\phi(x,t)$ after the sign reversal of a high negative field applied to a linearly splayed profile with $\phi_1=1°$ and $\phi_2=179°$ for $t_-=20$ ms, to demonstrate the sharpness and higher speed of motion of the kink-antikink pair. (b) Similar to (a) except for initially uniform structure with $\phi_1=\phi_2=179.99°$, showing that in this case the kink and antikink are produced exactly at the same time and collide exactly at the center of the cell.

kinks. The dynamics for lower deviation $\phi_1=1°$ and $\phi_2=179°$ is shown in Fig. 10 for the same fields used in the single soliton case of Figs. 5(d)–5(f).

For higher fields, the two kinks form more quickly, become sharper, and travel more quickly. It seems that they travel with higher velocity than the single soliton case. This fact is of particular interest because from the behavior of the velocity for the single-kink case with the field we expect the double-kink velocity to be smaller since $\delta\neq 0$. The only explanation we have is that the interaction between the kink and the antikink is attractive. Physically, this is because the nonswitched dipoles in the region between the kink and the antikink have orientations ϕ higher than those in the single kink case. In the later case, the nonswitched dipoles tend to stay at $\phi=0$ due to the fixed dipoles (with $\phi_1=0$) at the boundary $x=0$. That is, the delay time of the nonswitched dipoles in the kink-antikink case is shorter and it becomes shorter still as the kink-antikink approach each other until they collide. Hence, the higher the orientations ϕ_1 and ϕ_2, the faster the speed is of the kink-antikink pair. This is demonstrated in Figs. 9(b), 10(c), and 11(b) which correspond to the same field but different orientations $\phi_1=30°$, 1°, and 179.99°, respectively. In addition, the overall switching time of the cell is shorter than the single-kink case because in the double-kink case the distances traversed by each kink are shorter than the total thickness of the cell. The case of Fig. 11(b) represents an initially uniform cell with orientation $\phi_1=\phi_2=179.99°$. In this case the kink and antikink are formed at the same time, propagate in opposite directions with the same speed and collide exactly in the center of the cell.

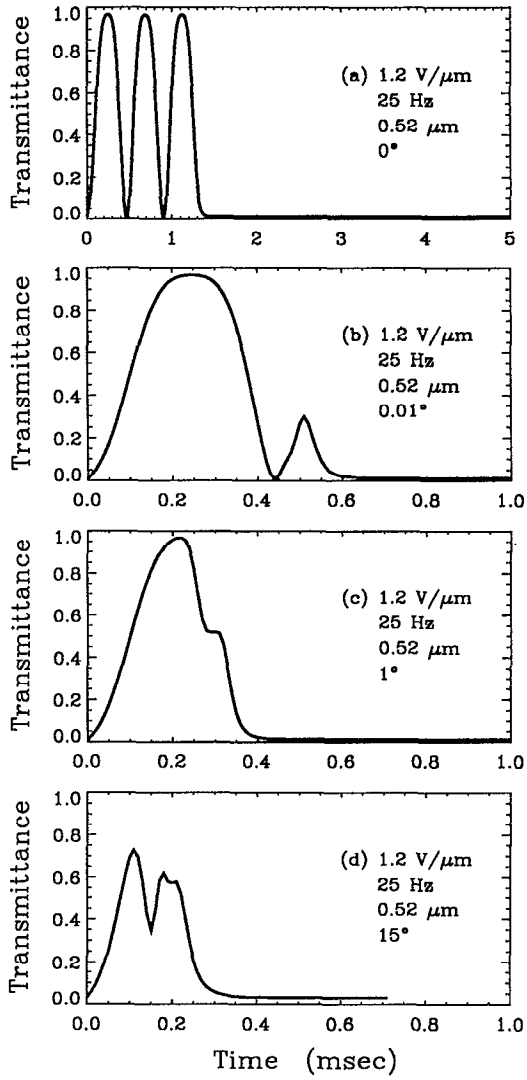

FIG. 12. The transient EO response associated with the motion of a single soliton when (a) $\phi_1=\theta$ and $\phi_2=\pi$ and (b)–(d) with the motion of kink-antikink pair when $\phi_1\neq 0$, $\phi_2=\pi-\phi_1$ for different values of ϕ_1. This figure demonstrates the strong effect of the fixed boundary dipole orientations on the EO response. The case with $\phi_1=1°$ exhibits one nearly pure transient peak and it explains the experimental observations.

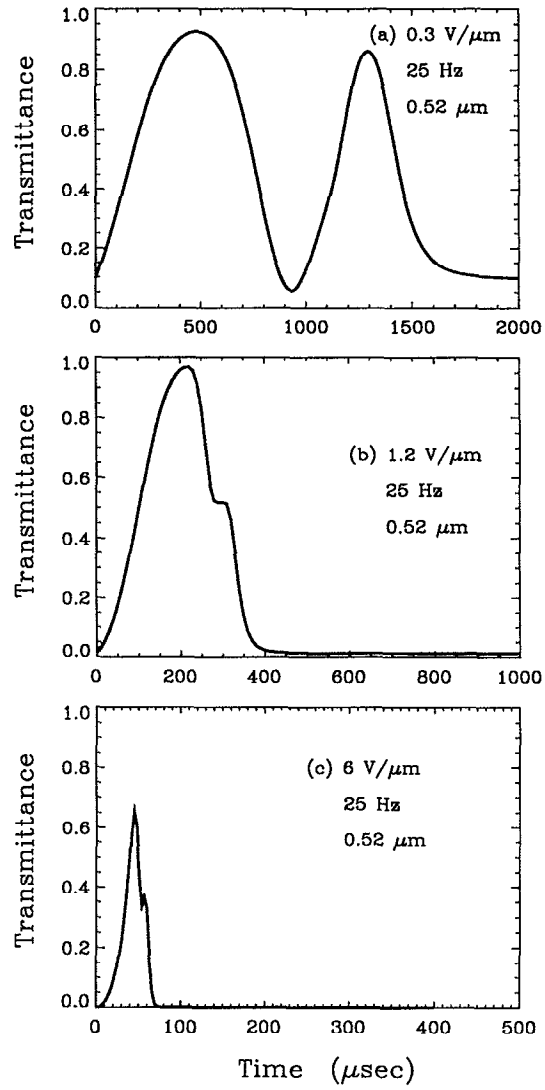

FIG. 13. The transient EO response associated with the motion of kink-antikink pair at different fields for $\phi_1=1°$, $\phi_2=179°$, and $\lambda=0.52$ μm satisfying the MFWP condition. At $E=1.2$–1.3 V/μm the pure transient peak reaches its maximum transmission value, then it decreases and saturates. This agrees with the experimental observations in Fig. 3(a). The transient transmittance pattern at low fields in (a) can become structured. (See Fig. 12.)

VI. EO RESPONSE ASSOCIATED WITH KINK-ANTIKINK EXCITATION

The transient EO response associated with the switching via the excitation of kink-antikink pairs with different values of ϕ was calculated using the same procedure described in Sec. IV. Figure 12 shows the transient transmittance for the $\Omega=0$ geometry and λ that satisfies the MFWP condition, demonstrating the drastic effect of the orientation ϕ_1 on the EO response. The three peak pattern [Fig. 12(a)] which corresponds to the single soliton case starts to distort as ϕ_1 increases. As we have shown in Sec. IV that the appearance of these peaks occurs at certain positions of the single kink, then the number of the nondistorted peaks depend on how far the right-hand-side kink has traveled before the left-hand-side kink (antikink) starts to form. Therefore, the distortion of the three peak pattern depends on ϕ_1 and the field when $\phi_1>0$. For $\phi_1=0.001°$ and $E=1.2$ V/μm the third peak [the one which appears last in Fig. 12(a)] distorts slightly. For $\phi_1=0.005°$ it disappears completely and the second peak starts to distort. For $\phi_1=0.01°$ the second peak is only 20% of the first and it disappears completely when $\phi_1=1°$, leaving one peak. For $\phi_1>1°$ this one peak pattern starts to distort again [Fig. 12(d)].

Hence, the case of having the boundary dipole orientation be slightly off ($\phi_1\sim 1°$) the normal to the substrates appears to be the most likely to occur. To support this prediction, the dependence of the single-peak pattern on the different parameters must be considered. Figure 13 shows the field dependence for the case of $\phi_1=1°$ and $\lambda=0.52$ μm. In the high-field regime the single pure peak persists but

becomes narrower in time, decays, and saturates above a certain field. In the low-field regime the pattern is more structured [Fig. 13(a)] but at very low fields a pure dip starts to appear. The transition from the structured pattern case to the pure dip case is shown in Fig. 14. Note that Figs. 14(a) and 14(b) are similar to those obtained in Figs. 7(a) and 7(b), respectively, for the single-kink case. This is because in the low-field regime for small ϕ the transient profiles $\phi(x,t)$ are similar. The structured pattern case has been also observed experimentally (not shown) and it always appears at fields between the cases of pure peak and pure dip. Nevertheless, the case of small fields can experimentally exhibit a complicated pattern, different from the calculated ones because this case is very sensitive to the initial as-prepared structure.

The variation of the single pure peak pattern with the wavelength is shown in Fig. 15 for the two geometries $\Omega=0$ and $\Omega=\theta$. Figures 15(a)–15(c) ($\Omega=0$ geometry) show the transition from the single pure peak pattern to the pure dip pattern as λ changes from the MFWP to satisfy the MHWP condition. This behavior is in excellent agreement with the observations [Fig. 3(b)]. Figures 15(d)–15(f) ($\Omega=\theta$ geometry) show the transition from the pure peak to the usual EO response behavior, in agreement with the observations in Figs. 2–4. Note that the existence and the shape of the pure peak does not depend on the cell orientation [Figs. 15(a) and 15(d)]. The only differences are in the peak height, in agreement with the observations shown in Figs. 2–4. Figure 16 shows excellent agreement between the measured and calculated values of the pure peak height versus the field strength.

The pure peak case can be understood in the high-field regime if we consider the cell to be composed of three parts of thicknesses d_1, d_2, and d_3 with their optical axis orientations being at $\phi=\pi$, 0, and π respectively. The thicknesses d_1 and d_3 are the distances traversed by the antikink and the kink respectively and hence $d_2=d-d_1-d_3$ is the nonswitched central part of the cell.

Using Jones calculus, the transmittance between crossed polarizers with $\Omega=0$ geometry is given by

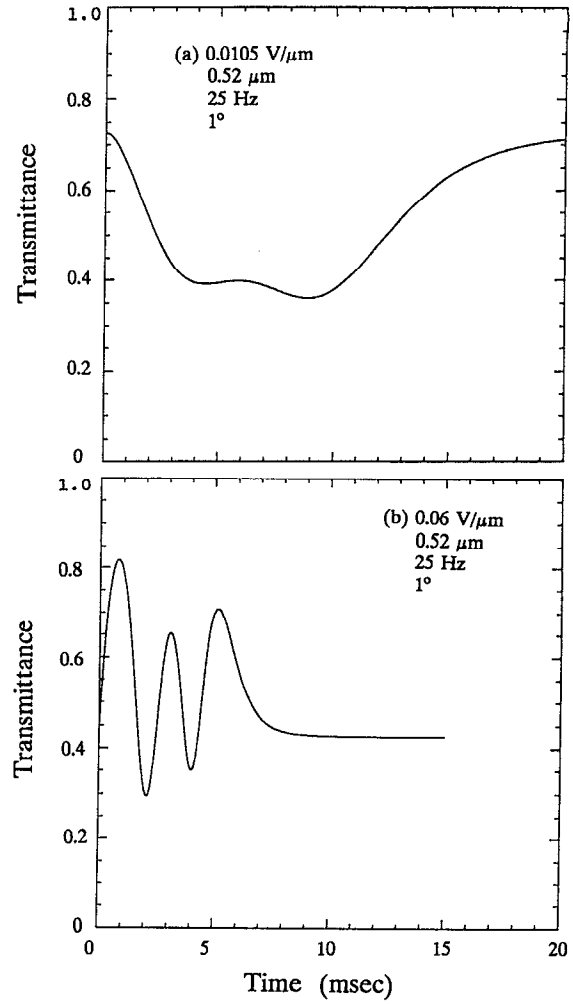

FIG. 14. The change of the transient EO response with the field in the low-field regime with the same conditions as in Fig. 13. At very low fields a pure transient dip is obtained as expected, but at intermediate fields the transmittance pattern can be structured.

$$T=\sin^2 2\theta(\{\cos(\Gamma_3/2)\sin(\Gamma_2-\Gamma_1)/2+\cos 4\theta\,\sin(\Gamma_1/2)\sin(\Gamma_2/2)\sin(\Gamma_3/2)-\sin(\Gamma_3/2)\cos[(\Gamma_1+\Gamma_2)/2]\}^2$$
$$+\cos^2 2\theta\{2\cos(\Gamma_3/2)\sin(\Gamma_1/2)\sin(\Gamma_2/2)-\sin(\Gamma_3/2)\sin(\Gamma_2-\Gamma_1)/2-\sin(\Gamma_3/2)\sin[(\Gamma_1+\Gamma_2)/2]\}^2), \quad (7)$$

where $\Gamma_{1,2,3}=(2\pi\Delta n_m/\lambda)d_{1,2,3}$. This expression can be simplified if we note that $\Gamma_2=\Gamma-\Gamma_1-\Gamma_3$, where $\Gamma=2\pi d\Delta n_m/\lambda$ which equals $2m\pi$ ($m=1,2,3,...$) for λ satisfying the MFWP condition, and using the fact that in the high-field regime $\Gamma_1\approx\Gamma_3$ at any time during the switching. The simplified result is

$$T\approx\sin^2 2\theta\{[\cos(\Gamma_3/2)\sin(3\Gamma_3/2)\pm\tfrac{1}{2}\sin\Gamma_3]^2$$
$$+\cos^2 2\theta[\sin^2\Gamma_3-\sin(\Gamma_3/2)\sin(3\Gamma_3/2)$$
$$-\sin^2(\Gamma_3/2)]^2\}, \quad (8)$$

where the ($\pm$) signs correspond to m being odd or even, respectively. Since $\theta=\pi/8$ then for $\Gamma_3=(2n-1)\pi$ ($n=1,2,...$), we have $T=100\%$ and for $\Gamma_3=2n\pi$ we have $T=0\%$. This is a similar result to the single soliton case. However, in the double-kink case we have $d_3<d/2$ or $\Gamma_3<\Gamma/2$ which imposes an upper limit on the maximum number of peaks which is $n_{\max}<(m+1)/2$. For $\lambda=0.52$, $\Delta n_m=0.16$, and $d=10$ μm we have $m=3$ and hence $n_{\max}<2$, that is, more likely to have one transient peak, i.e., $n_{\max}=1$. As is seen in Fig. 12, the transient pattern can become complicated depending on the value of ϕ_1. This complex structure is believed to be due to the nonuniform layers formed both in the initial stages of the switching and also

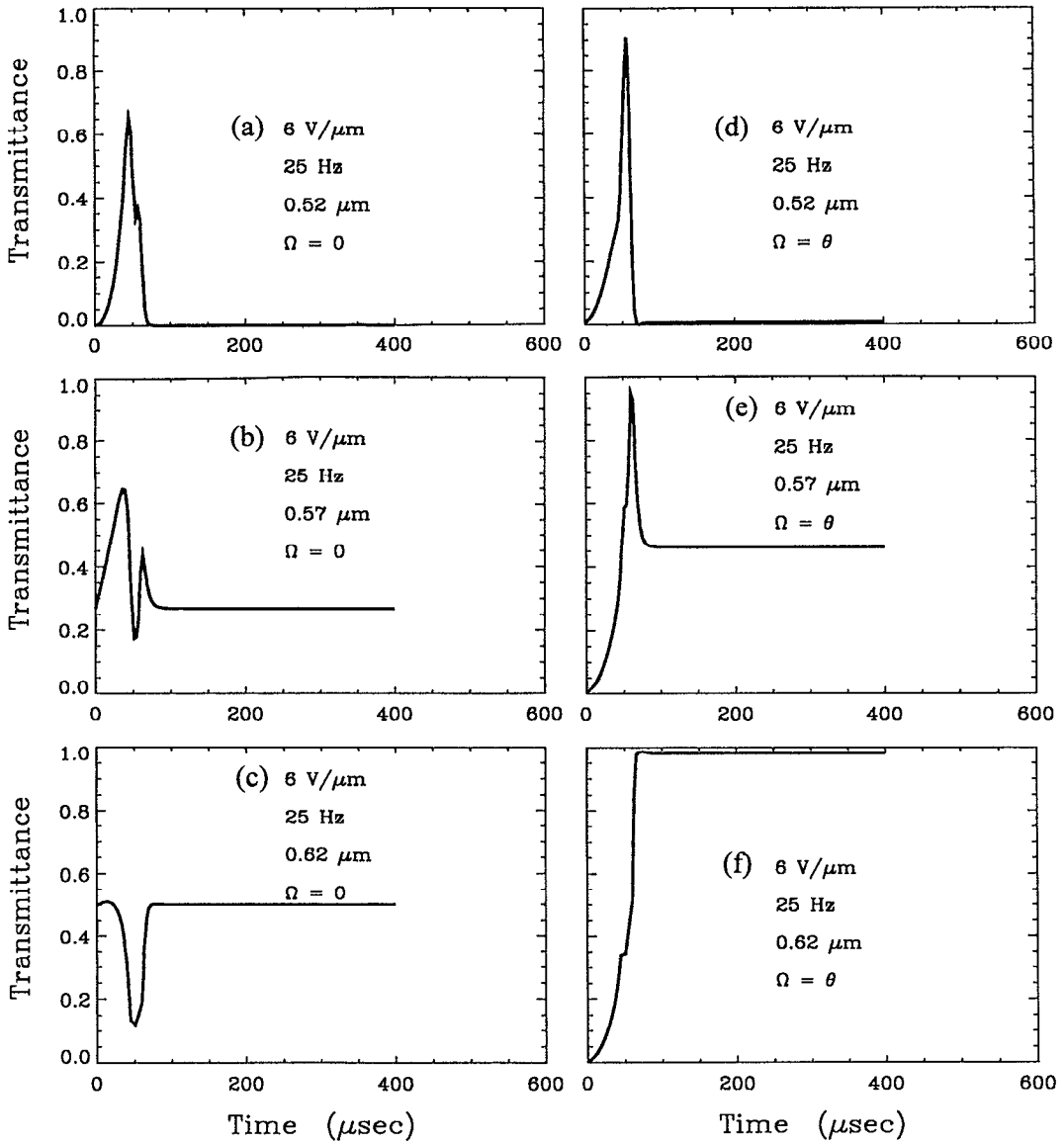

FIG. 15. (a)–(c) The transient EO response for the same conditions as in Fig. 14 in the high-field limit at different wavelengths. (a)–(c) show the transition from a pure transient peak at λ satisfying the MFWP condition to a pure dip for λ satisfying the MHWP condition in the geometry Ω=0. (a)–(c) explain the observations in Fig. 3(b), and also demonstrate the dependence of the transient EO on the cell orientation at different wavelengths, in agreement with the observations. (d)–(f) Similar to (a)–(c) but for the Ω=θ geometry. The response undergoes a transition from a pure transient peak at λ satisfying the MFWP condition to the usual EO response when λ satisfies the MHWP condition. (d)–(f) explain the observations in Fig. 2(a).

due to the finite width of the domain walls. Although in the high-field limit the width of the domain walls becomes small, the domain walls still can alter the phase of an electromagnetic field propagating through them, in particular in the visible range of the spectrum. Nonuniform splayed layers of FLCs have been found recently to alter the EO response drastically.[10]

VII. CONCLUDING REMARKS AND SUMMARY

The switching behavior of ferroelectric liquid crystals with fixed boundary dipole orientations was investigated both theoretically and experimentally. Experimentally, the EO response of FLC under bipolar field consists of a transient transmittance peak appearing when the wavelength of light is close to satisfying the multi-full-wave-plate condition. The shape, height, and the behavior of this transient peak with the field strength and the cell orientation cannot be explained using the simplified picture of switchable birefringent plate. That is, the case of having FLC structures with the boundary dipole orientations being free to reorientate is excluded. The possibility of explaining this behavior according to the transient scattering associated with ferroelectric domains reversal is also excluded due to the different behavior with various parameters.

The existence of transient nonuniform structures during the switching is found to be the only possible explanation. In order for these nonuniformities to persist at any field, the dipole orientations at the boundaries have to be fixed and not influenced by the maximum field which is applied. When the boundary dipoles are fixed exactly along the normal to the

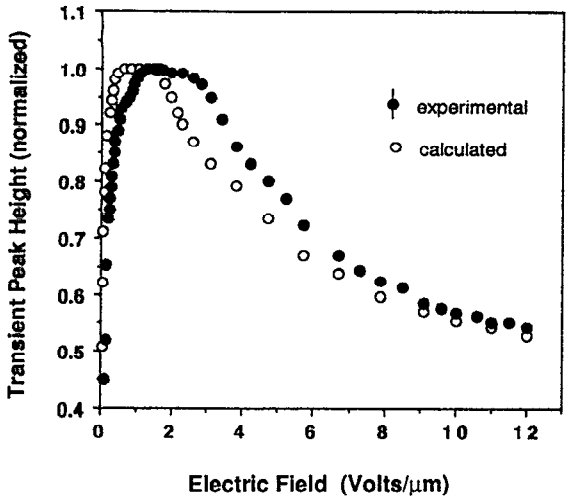

FIG. 16. Experimental and theoretical behavior of the pure transient peak height with the applied field in the $\Omega=0$ geometry and λ satisfying the MFWP condition. The theoretical values were obtained from calculations similar to those presented in Figs. 13(a) and 13(c) with $\phi_1=1°$ and $\phi_2=179°$.

substrates, theoretically the director-polarization reorientation proceeds via the creation of a single soliton moving at constant velocity v from one boundary to the other. In this case the transient EO response is that of two birefringent plates having thicknesses vt and $d-vt$ with their optic axis orientated at an angle 2θ with respect to each other. The transient EO response in this case consists of maxima and minima. When λ satisfies the multi-full-wave-plate condition of order m the number of peaks is equal to m. When the field increases, the peaks become narrow but their height stays equal to 100%. This behavior does not explain the experimental observations.

When the boundary dipole orientations are off the normal to the substrates the switching proceeds via the excitation of a kink-antikink pair near the boundaries, propagating in opposite directions, and colliding near the center of the cell. We found that small deviations ($\phi_1<1°$) of the dipole orientations from the surface normal alters the EO response drastically. The case which explains the experimental observations nicely is the one with $\phi_1\sim1°$. The transient EO response in this case consists of one peak which becomes narrower with the field, with a height that reaches a maximum at a certain field, and then decays and saturates.

The generality of the experimental observations to many FLC mixtures prepared by different alignment techniques suggests that a fundamental reason exists for the boundary dipoles to be orientated slightly off the normal to the substrates. We note that this small deviation of the boundary dipoles $\phi_1\sim1°$ is of the same order of magnitude of the thermal fluctuations according to the mean field theory.[4] If these fluctuations did exist in the bulk we would expect the shape of the moving domain walls during the switching to change randomly in time. The associated EO response would then be different from the observations. Therefore, we suggest that the amplitude of the thermal fluctuations is much smaller than 1°. One possible cause for that is the strong anchoring to the substrates, which can quench the fluctuations over all the cell thickness. Such a calculation of the amplitude of the fluctuations which includes the effect of the anchoring has not been reported to our knowledge. Additional effects, such as the flow, reveal additional characteristics and are being considered.[13]

The experimental observations described in this article represent the general behavior of the transient EO response of FLCs. As mentioned earlier, differences in the behavior of different cells do exist, possibly due to defects, asymmetry in the anchoring energy at the two surfaces, flow and fluctuation effects, and the existence of ions or impurities. We have found that by fitting the calculated transient EO response to a bipolar field to experimental observations we have been able to characterize successfully the switching of FLCs, and suggest that the technique be extended to include additional effects.

[1] J. W. Goodby, R. Blinc, N. A. Clark, S. T. Lagerwall, M. A. Osipov, S. A. Pikin, T. Sakurai, K. Yoshino, and B. Zeks, *Ferroelectric Liquid Crystals. Principles, Properties and Applications*, Ferroelectricity and Related Phenomena Series Vol. 7 (Gordon and Breach, New York, 1991).
[2] I. Abdulhalim, G. Moddel, and N. A. Clark, Appl. Phys. Lett. **60**, 551 (1992).
[3] K. Yoshino and M. Ozaki, Ferroelectrics **59**, 1451 (1984).
[4] J. E. Maclennan and N. A. Clark, Phys. Rev. A **44**, 2543 (1991).
[5] J. E. Maclennan, N. A. Clark, and M. A. Handschy, in *Solitons in Liquid Crystals*, edited by L. Lam and J. Prost (Springer, New York, 1991), pp. 151–190.
[6] R. M. Sincovec and N. K. Madsen, A. C. M. Trans. Math. Software **1**, 232 (1975).
[7] A. Seeger and P. Schiller, in *Physical Acoustics*, edited by W. P. Mason, (Academic, New York, 1966), Vol. III, Part A, pp. 361–493.
[8] P. Schiller, G. Petzl, and D. Demus, Liquid Cryst. **2**, 21 (1987).
[9] I. Abdulhalim, Optics Commun. (in press).
[10] I. Abdulhalim, Europhys. Lett. **19**, 91 (1992); **19**, 439 (E) (1992).
[11] D. W. Berreman and T. J. Scheffer, Phys. Rev. Lett. **25**, 577 (1970).
[12] I. Abdulhalim, L. Benguigui, and R. Weil, J. Phys. (Paris) **46**, 815 (1985).
[13] Z. Zou, T. Carlsson, and N. A. Clark, in 14th International Liquid Crystal Conference, Pisa, Italy, June 21–26, 1992.